EIGEN-ANALYSIS OF A CANTILEVERED FLEXIBLE PLATE IN CHANNEL FLOW

A.D. Lucey & M.W. Pitman
Fluid Dynamics Research Group, Curtin University of Technology, Perth, Australia
R.M. Howell
Fluid Dynamics Research Centre, University of Warwick, Coventry, U.K.

ABSTRACT

A new computational model is developed and used to conduct a comprehensive study of the two-dimensional linear stability of a cantilevered flexible plate in uniform flow. Boundary-element and discrete-vortex methods are used to model the flow field. The plate is described by a finite-difference form of the beam equation. Stability is assessed by casting the system equation in State-Space form and directly extracting the eigenmodes. We also perform numerical simulations to expose the cause and nature of system instabilities. We show that, as flow speed is increased, short plates succumb to single-mode flutter caused by irreversible energy transfer while the critical instability for long plates is similar to the Kelvin-Helmholtz type of modal-coalescence associated with the flutter of panels held at both ends. Within this framework, the effects of plate length, an upstream rigid splitter plate, channel-wall proximity, and the wake are evaluated and interpreted.

1. INTRODUCTION

The linear stability of the two-dimensional system illustrated by Fig. 1 is studied. While this system is of fundamental interest, the phenomenology of its dynamics also underlies the behaviour of many physical systems ranging from fluttering flags, to oscillations of the human soft-palate that create snoring noises, and to energy-harvesting devices that could extract fluid energy through its transfer to the plate in a process of controlled destabilization.

The early paper of Kornecki *et al.* [1] is perhaps the starting point for interest in the problem at hand. Using ideal flow they studied a flexible plate embedded in an infinite domain of fluid, as did the recent work of [2-5]. This fundamental configuration has been extended to that of a flexible plate mounted in plane channel flow [6-9]. These studies predict that the plate loses its stability through flutter that sets in beyond a critical uniform flow speed or Reynolds number in the case of viscous channel flow [8,9]. For short plates the flutter mode is predicted to comprise a combination of the first and second *in-vacuo* modes while for long plates, or plates with heavy fluid loading, the critical mode is dominated by higher-order modal content. While the methods of this paper serve to reproduce many of these findings, a key contribution of our work is to provide an exposition of instability mechanisms. Through this understanding, we are then able to provide a clearer interpretation of the quantitative effects caused by refinements to the Kornecki-system such as the inclusion of a rigid splitter-plate mounted upstream of the flexible plate, channel walls, and the vortical wake that is shed from the trailing edge of the plate (see also [10]).

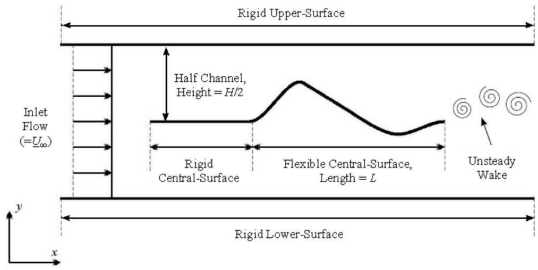

Figure 1: Schematic of the fluid structure system studied.

2. METHODS

The irrotational part of the flow field is found using a linearised boundary-element method (BEM) while the vorticity shed from the trailing edge of the flexible plate is modelled using the discrete-vortex method (DVM). In the application of the BEM, second-order vortex panels are used on the rigid central surface and the

flexible plate because of the discontinuity of tangential fluid velocity across these surfaces; they can therefore be considered as lifting surfaces. It is the distributed lift that drives the motion of the flexible plate. Source-sink panels are applied on the rigid channel walls. A schematic of the scheme is shown in Fig. 2. The singularity strengths are determined by enforcing the no-flux boundary condition at every panel control point and, for the central surfaces, continuity of the distributed vorticity between adjacent panels. Thus the vector of singularity strengths is given by

$$\{\Gamma_m\} = \left[I_{im}^N\right]^{-1} \left\{U_\infty \theta_m + \dot{\eta}_m + u_m^{Nb}\right\}, \quad (1)$$

where $\Gamma_m = \gamma_m + \lambda_m$ for the vortex elements. $\left[I_{im}^N\right]^{-1}$ contains, in addition to the normal influence-coefficients of the singularities, the boundary conditions of: a) vortex strength continuity at panel end points; and b) zero vorticity at the plate's trailing edge (thus enforcing the standard Kutta condition for linear displacements of zero pressure difference at the trailing edge). θ_m is the panel's angle to the horizontal, which in the linear framework is the streamwise spatial derivative of the boundary, η_m, while u_m^{Nb} is the normal component of the velocity induced by the wake vortices evaluated at control point m.

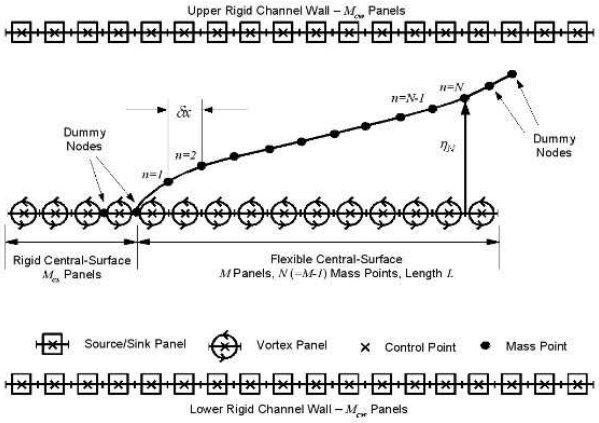

Figure 2: Summary of elements used in the flow-field computational model.

The unsteady Bernoulli equation is used to determine the pressure distribution on the flexible plate. The transmural pressure is then used as the forcing term in the one-dimensional thin flexible-plate equation couched in finite-difference form. The motion of the plate and the fluid flow are fully coupled through deflection, vertical velocity and acceleration of the two media at their interface. For the vortical wake, Gaussian vortex blobs are shed at each time-step of the plate's motion; the circulation assigned to each blob is such that Kelvin condition is enforced. Linearised convection is adopted in the present study whereby the blob centres remain in the horizontal plane of the undisturbed plate and thus travel downstream only with the speed of the mean flow. This approach allows a single system (matrix) equation to be written as follows.

$$\begin{aligned} \rho h \left[\mathbf{I}\right]\{\ddot{\eta}_m\} + d\left[\mathbf{I}\right]\{\dot{\eta}_m\} + B\left[\mathbf{D_4}\right]\{\eta_m\} = \\ 2\rho_f U_\infty^2 \frac{1}{\delta x}\left[\mathbf{B_1^+}\right]\{\eta_m\} + \rho_f \dot{U}_\infty \frac{1}{\delta x}\left[\mathbf{B_2^+}\right]\{\eta_m\} \\ +\rho_f U_\infty \frac{1}{\delta x}\left[\mathbf{B_2^+}\right]\{\dot{\eta}_m\} + \rho_f U_\infty \left[\mathbf{B_1^-}\right]\{\dot{\eta}_m\} \\ +\rho_f \left[\mathbf{B_2}\right]\{\ddot{\eta}_m\} \\ -2\rho_f U_\infty \left[\mathbf{B_1}\right]\left\{u_m^{Nb}\right\} - \rho_f \left[\mathbf{B_2}\right]\left\{\dot{u}_m^{Nb}\right\}, \end{aligned} \quad (2)$$

where $[\mathbf{B}]$ are matrices of singularity influence coefficients, $[\mathbf{D_4}]$ is a fourth-order spatial-differentiation matrix and $[\mathbf{I}]$ is the identity matrix. ρ, h, d and B are respectively, the material density, thickness, dashpot-type damping coefficient and flexural rigidity of the plate, the dynamics of which appear on the left-hand side of the equation. The pressure perturbation that drives the plate motion appears on the right-hand side, where ρ_f and U_∞ are the fluid density and flow speed, noting that our formulation permits a time-dependent uniform flow to be used. The pressure terms in the line order of Eqn. 2 can be interpreted in the following way: Line 1 contains the deflection-based hydrodynamics stiffness plus a deflection-based cross term arising from an unsteady mean flow; Line 2 contains the plate-induced hydrodynamic damping; Line 3 contains the plate-induced hydrodynamic inertia; and Line 4 comprises the respective contributions to hydrodynamic damping and inertia from the wake vorticity.

We take two approaches to the solution of Eqn. 2. Neglecting the wake-vortex contributions it becomes a second-order differential equation in $\{\eta\}$. Setting $w_1(t) = \eta(t)$ and $w_2(t) = \dot{\eta}(t)$ and rearranging the matrices in companion-matrix form, yields a system equation in the form

$$\dot{w} = [H]w, \quad \text{where} \quad w = \{w_1, w_2\}^T \quad . \quad (3)$$

Single-frequency time-dependent response is assumed at ω which is a complex eigenvalue of $[H]$. Positive ω_I and ω_R respectively represent the oscillatory and amplifying parts of the response, the eigenvector of which is readily assembled. However, we note that this approach

can be adapted to include wake effects. This requires an additional set of N_W variables, $\{\omega\}$, to be defined as being the discrete vorticity on an Eulerian grid in the wake; in the linear assumption the grid simply becomes a line. The inclusion of a further N_W unknowns requires the enforcement of the vorticity transport equation in the wake to close the system. The steady Kutta condition at the trailing edge is replaced by a condition of continuous vorticiy shedding. This results in the fluid-strucute system being cast in the form a first-order differential equation for the vector of unknowns $\{\eta, \dot{\eta}, \omega\}^T$ that yields a linear eignevalue problem.

Alternatively, we perform a time-discretisation of η in Eqn. 2 and then numerically time-step, using a semi-implicit method, the equation to determine the system response to some form of initial or continuing applied excitation. In doing so we are able to study transient behaviour and reveal localsied flow-structure dynamics that when summed contribute to the system response.

3. RESULTS

We non-dimensionalise using the scheme in [11,12] and thus

$$\bar{t} = t\ [\rho_f^2 B^{\frac{1}{2}}/((\rho h)^{\frac{5}{2}})],\ \ \bar{U} = U_\infty\ [(\rho h)^{\frac{3}{2}}/(\rho_f B^{\frac{1}{2}})]$$
$$\text{and} \qquad \bar{d} = d\ [(\rho h)^{\frac{3}{2}}/(\rho_f^2 B^{\frac{1}{2}})]. \qquad (4a,b,c)$$

However, angular frequencies are presented as a ratio to the frequency of the second *in-vacuo* plate mode instead of using the time scale that appears in Eqn. 4a; this allows a better physical grasp of the effect of the fluid loading and accounts for the length of the plate. The non-dimensional length (or mass ratio) of the flexible plate and the channel height are defined by

$$\bar{L} = L[\rho_f/(\rho h)] \quad \text{and} \quad \bar{H} = H[1/L]. \quad (5a,b)$$

3.1. Standard case

Figure 3 shows the variation of system eigenvalues with applied flow speed for a short plate, $\bar{L} = 1$, effectively, in the absence of channel walls for which, $\bar{H} = 1$ is sufficiently large as demonstrated by numerical experiments, and with no upstream splitter plate. For the case of an elastic plate that generated Fig. 3a, these results compare well with the corresponding results in [7]. Single-mode flutter of the second system mode, is the critical instability at a non-dimensional flow speed given by $\bar{U} = U_c = 5.452$. The inclusion of dissipation in the same system through structural damping with a coefficient $\bar{d} = 5$ yields the result of Fig. 3b. The critical flow speed is now higher and this strongly indicates that the instability is driven by irreversible energy transfer from the fluid to the plate. This has been confirmed by monitoring the phase angle between the pressure loading and plate velocity in numerical simulations. Both the leading-edge singularity and the trailing-edge Kutta condition contribute to non-orthogonality of the pressure and plate velocity. The product of these terms yields the localised rate of work done (per unit area of plate) which is then non-zero when integrated over one period of oscillation, both locally and when summed to obtain the energy record of the entire plate.

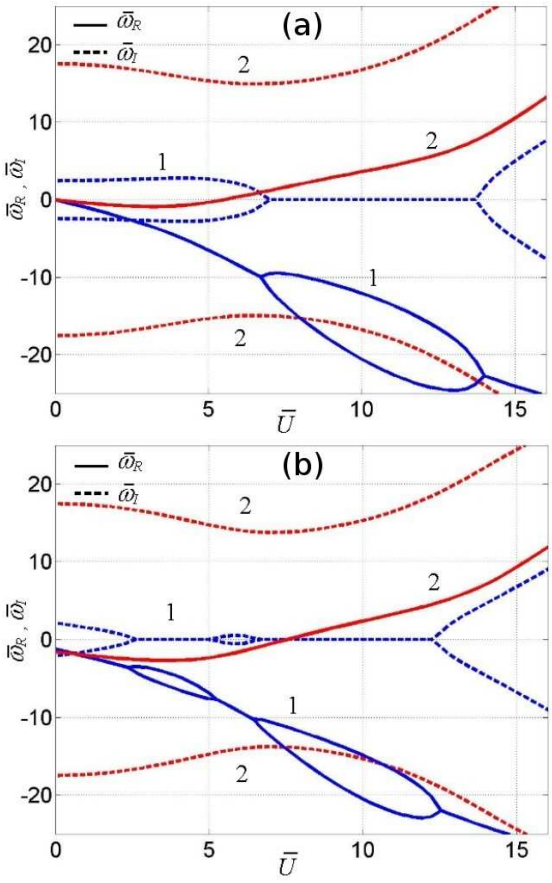

Figure 3: Fluid-structure behaviour at $\bar{L} = 1$, $\bar{H} = 1$ (effectively isolated): Variation of system eigenmodes with flow speed where (a) elastic plate, $\bar{d} = 0$, and (b) including structural damping with $\bar{d} = 5$. In this and subsequent eigenvalue plots, the numbers on each figure identify the mode number in order of ascending frequency at $\bar{U} = 0$

Figure 4b shows the energy record during the numerical simulation of the critical mode, the

motion of which is presented in Fig. 4a. Note that the simulation is commenced by releasing the plate from an applied deformation - the thick black line - in the shape of second *in-vacuo* mode. The critical mode, seen to contain strong contributions from the first and second *in-vacuo* modes, then evolves from the initial excitation. The sum of energy transferred from fluid to plate in Fig. 4 shows that energy exchanges are spatially dependent; thus for example, the third quarter from the leading edge of the flexible is locally unstable while the fourth quarter is stable. It is the sum of of all these energy transfers that, in this case, yields the neutral stability of the system.

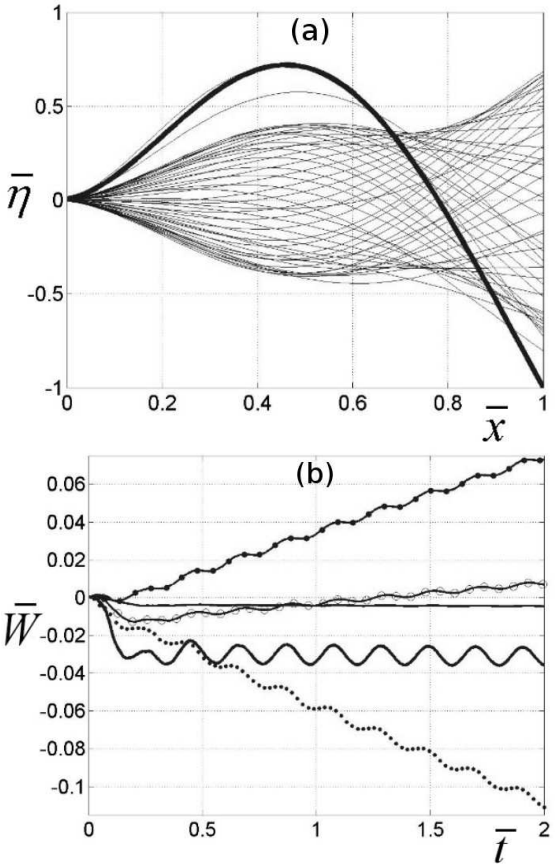

Figure 4: Fluid-structure behaviour at $\bar{L} = 1$, $\bar{H} = 1$ (effectively isolated): Numerical simulations of system behaviour with $\bar{d} = 0$ at the critical flow speed $U_c = 5.452$, (a) time-sequence of instantaneous plate deformation (the thick line is the initially imposed deformation), (b) time-variation of work done by fluid on plate with — (thin), –○–, –●–, ⋯ each respectively indicating total work done and spatial contributions from the first, second, third and fourth quarters of the plate from its leading edge.

3.2. Long plate

The effect of plate length (or fluid-to-plate density ratio) is demonstrated by Fig. 5, in which $\bar{L} = 10$, that can be compared directly with the short-plate result of Fig. 3a. Instability now sets in at approximately $\bar{U} = 0.63$ of the fluid-structure Mode 2. However, this is not a single-mode flutter. Instead, it is the result of modal coupling - an inexact modal-coalescence - with Mode 3 with Mode 2 having interacted with Mode 1 at lower flow speeds. This instability is the result of essentially conservative energy transfers in contrast to the irreversible energy transfer mechanism of single-mode flutter. Thus, for long plates, the phase-alignment between pressure and plate velocity is closer to the orthogonality that occurs for potential flow over an infinitely long flexible boundary.

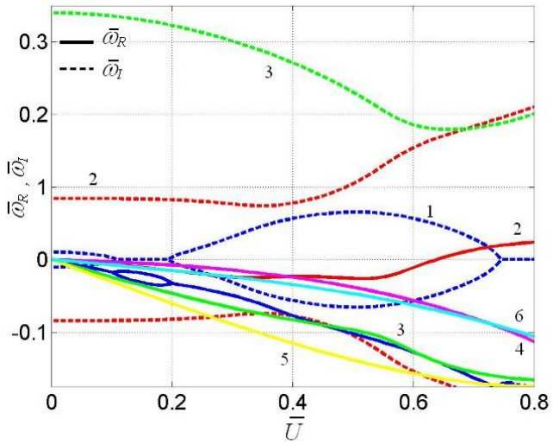

Figure 5: Fluid-structure behaviour at $\bar{L} = 10$, $\bar{H} = 1$ (effectively isolated): Variation of system eigenmodes with flow speed where $\bar{d} = 0$.

3.3. Effect of upstream splitter plate

A splitter plate, of length equal to $\bar{L} = 1$, is now introduced to the standard case. The resulting eigenvalues are shown in Fig. 6; these can be compared directly with the results in Fig. 3a. The critical speed rises from 4.452 to 13.547 and it is Mode 3 that is now critical. Inspection of Fig. 6 shows that, like the long plate of §3.2, it is the modal coalescence of Modes 2 and 3 that first destabilizes the plate with increasing flow speed. The splitter plate serves to distance the leading-edge singularity, a key contributor to the phase-relation effects of finiteness, from the flexible plate, thereby weakening the single-mode flutter mechanism. For this length of splitter plate the lower-speed single-mode flutter is

completely eliminated so that modal-coalescence instability yields the critical flow speed.

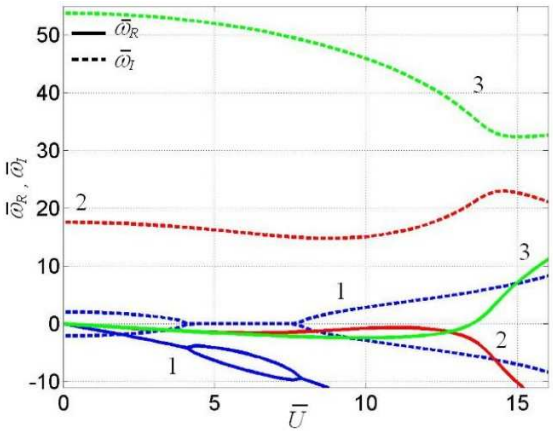

Figure 6: Fluid-structure behaviour at $\bar{L} = 1$, $\bar{H} = 1$ (effectively isolated) and splitter plate of length $\bar{L} = 1$: Variation of system eigenmodes with flow speed.

3.4. Effect of channel walls

The effect of channel walls, with $\bar{H} = 1$, is illustrated by the numerical simulation that generated Figure 7 in which the neutrally stable mode at the critical speed, $\bar{U} = U_c = 5.177$, is depicted. The critical flow speed is thus slightly decreased but in other respects the phenomenology is the same as that of the unbounded standard case of §3.1. The reduction to critical speed is caused by an intensification of the pressure forces due to the constraints imposed by the channel walls.

3.5. Effect of wake

The effect of channel walls, with $\bar{H} = 1$, is illustrated by the numerical simulation that generated Figure 7 in which the neutrally stable mode at the critical speed, $\bar{U} = U_c = 5.177$, is depicted. The critical flow speed is thus slightly decreased but in other respects the phenomenology is the same as that of the unbounded standard case of §3.1. The reduction to critical speed is caused by an intensification of the pressure forces due to the constraints imposed by the channel walls.

4. CONCLUSIONS

A new computational model has been developed for the interaction of cantilevered-free flexible plate with a low-speed potential flow. The model permits us to evaluate the effects on stability of channel-wall proximity, an upstream splitter

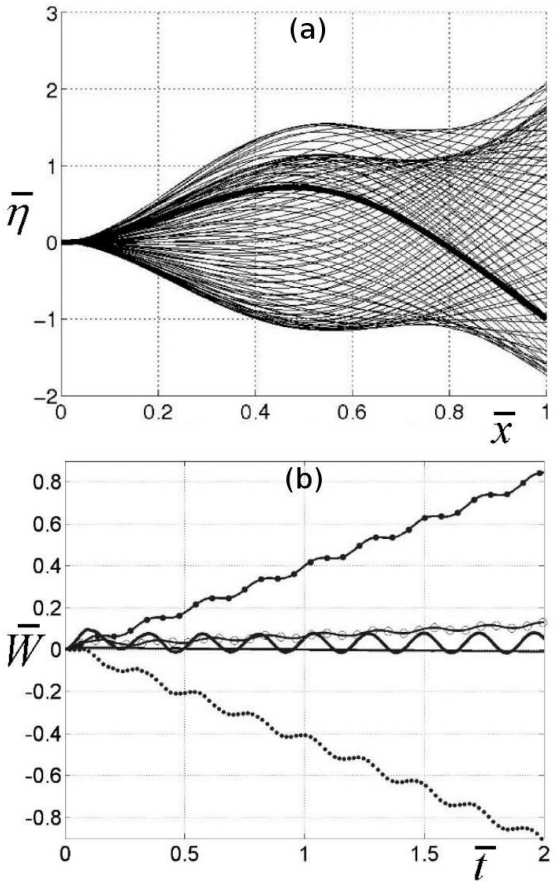

Figure 7: The effect of channel walls on the system response: Numerical simulation of system behaviour for$\bar{L} = 1$, $\bar{H} = 0.1$ and $d = 0$ at the new critical flow speed $U_c = 5.177$, (a) time-sequence of instantaneous plate deformation (the thick line is the initially imposed deformation), and (b) time-variation of work done by fluid on plate, W, line types same as in Figure 4b

plate and the wake that originates from the trailing edge of flexible plate. Direct extraction of the fluid-structure eigenvalues is permitted by the present mathematical formulation. Predictions of the infinite-time system response can therefore be made. We complement these by conducting numerical simulations of initial-value problems that additionally elucidate the localised responses that, when summed, yield the system response. We show that short plates are destabilsed by a single-mode flutter whereas long plates and plates with a suitably long upstream splitter plate are destabilised by modal coalescence flutter. While the effect of channel-wall proximity does not significantly modify the system response, the effect of a wake is stabilising for single-mode flutter but promotes modal-coalescence flutter.

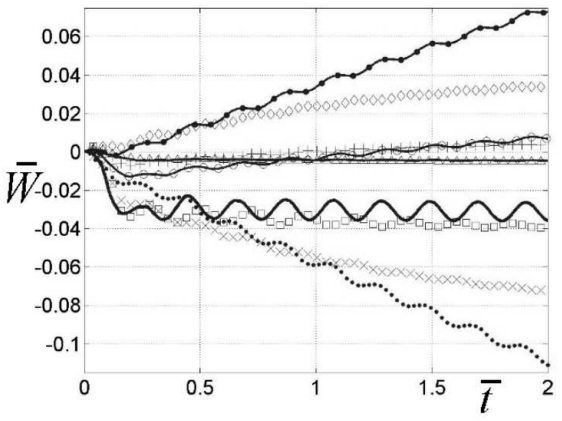

Figure 8: The effect of an unsteady wake on the system response. Numerical simulation at $\bar{L} = 1$, $\bar{H} = 1$ (effectively isolated) and $\bar{d} = 0$. Time variation of work done by fluid on plate, $\bar{W}$, with (discrete data) and without (continuous data) a wake at $\bar{U}_c = 5.452$ (the critical speed found without a wake). Where the data sequences $\triangle$, $+$, $\diamond$, $\times$ and — (thin), –○–, –●–, $\cdots$ each respectively indicate the work done over the first, second, third and fourth quarters of the plate from its leading edge, while □ and — (thick) are the respective sums of these contributions.

5. REFERENCES

[1] Kornecki, A., Dowell, E. H. & O'Brien, J. 1976 On the Aeroelastic Instability of Two-Dimensional Panels in Uniform Incompressible Flow. *Journal of Sound and Vibration*, **47**, 163–178.

[2] Huang, L. 1995 Flutter of Cantilevered Plates in Axial Flow. *Journal of Fluids and Structures* **9**, 127-147.

[3] Yamaguchi, N., Yokota, K. & Tsujimoto, Y. 2000a Flutter Limits and Behaviours of a Flexible Thin Sheet in High Speed Flow - I: Analytical Method for Prediction of the Sheet Behaviour. *Journal of Fluids Engineering* **122**, 65-73.

[4] Watanabe, Y., Isogai, K., Suzuki, S. & Sugihara, M. 2002b A Theoretical Study of Paper Flutter. *Journal of Fluids and Structures* **16**, 543-560.

[5] Argentina, M. & Mahadevan, L. 2005 Fluid-flow-induced flutter of a flag. *Proceedings of the National Academy of Sciences* **102**, 1829-1834.

[6] Aurégan, Y. & Depollier, C. 1995 Snoring: Linear Stability Analysis and *in vitro* Experiments. *Journal of Sound and Vibration* **188**, 39-54.

[7] Guo, C. Q. & Païdoussis, M. P. 2000 Stability of Rectangular Plates with Free Side-Edges in Two-Dimensional Inviscid Channel Flow. *Journal of Applied Mechanics* **67**, 171-176.

[8] Balint, T. S. & Lucey, A. D. 2005 Instability of a cantilevered flexible plate in viscous channel flow. *Journal of Fluids and Structures* **20**, 893-912.

[9] Tetlow, G.A., Lucey A.D. & Balint, T.S. 2006 Instability of a cantilevered flexible plate in viscous channel flow driven by constant pressure drop. In *Proceedings of ASME Pressure Vessels and Piping Division Conference, Vancouver, BC, Canada Paper no.: PVP2006-ICPVT11-93943.*

[10] Tang, L. & Païdoussis, M. P. 2007 On the instability and the post-critical behaviour of two-dimensional cantilevered flexible plates in axial flow. *Journal of Sound and Vibration* **305**, 529-542.

[11] Crighton, D.G. & Oswell, J.E., 1991, Fluid loading with mean flow. I. Response of an elastic plate to localized excitation. *Philosophical Transactions of the Royal Society of London A*, **335**:557-592.

[12] Lucey, A.D., 1998, The excitation of waves on a flexible panel in a uniform flow. *Philosophical Transactions of the Royal Society of London A*, **356**:2999-3039.